

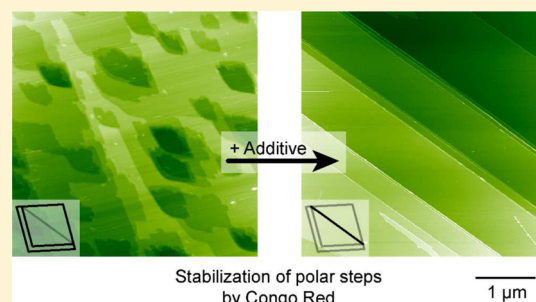
Stabilization of Polar Step Edges on Calcite (10.4) by the Adsorption of Congo Red

Rebecca Momper, Martin Nalbach, Karin Lichtenstein, Ralf Bechstein, and Angelika Kühnle*

Institute of Physical Chemistry, Johannes Gutenberg University Mainz, Duesbergweg 10-14, 55099 Mainz, Germany

Supporting Information

ABSTRACT: In this work, we present the stabilization of polar step edges along the [010] direction of calcite (10.4) by the presence of a water-soluble organic molecule, namely Congo Red. While characteristic etch pits are observed on the surface in the absence of the additive, no etch pits can be found in the presence of the additive. Using atomic force microscopy, we can directly follow the restructuring of the surface. Upon addition of Congo Red, the charge-neutral step edges confining the characteristic etch pits vanish, while polar step edges along the [010] direction appear on the surface, which are entirely decorated by well-ordered molecular islands of the additive. After the restructuring has taken place, the surface exclusively exhibits these polar step edges. Our results give direct evidence of the fact that these polar step edges become thermodynamically favored when Congo Red is present.



INTRODUCTION

Additive-controlled crystallization¹ is pivotal in many processes in both nature and industry. Especially in chemical, pharmaceutical, and food industries, crystallization processes are often controlled by the presence of suitable additives and sophisticated processing conditions.² Despite their extensive use, however, the mode of action of soluble additives remains largely unknown and empirical recipes are frequently improved by trial and error.

Especially calcite^{3,4} has attracted considerable attention in the context of additive-controlled crystallization, as this major rock-forming mineral plays an important role in many geochemical and biological and industrial processes. Within industry, additives are frequently used for the inhibition of nucleation and crystal growth of calcite, e.g., in seawater desalination and scale inhibition. Moreover, understanding the mechanisms governing additive-controlled calcium carbonate crystallization is of fundamental interest within biomineralization.⁵

Consequently, the impact of organic additives on dissolution and growth of the thermodynamically most stable cleavage plane of calcite, calcite (10.4), has been studied extensively, including organic additives such as amino acids,^{6,7} peptides,⁸ proteins, and ancient polysaccharides.⁹ In these studies, atomic force microscopy has been used as an unparalleled tool^{10–13} to directly visualize the morphological changes induced by the presence of soluble additives in real space. In an extensive study by Nelea et al.,⁸ the effect of the negatively charged protein osteopontin on the morphology of the characteristic etch pits on the calcite (10.4) surface has been investigated. Besides the thermodynamically most stable step edges along the [4–4–1] and [48–1] substrate directions, a variety of other steps

including polar step edges along the [010] direction could be observed in that study.

Additives can influence dissolution and growth in different ways. On one hand, molecules can bind to specific sites on the surface, e.g., negatively charged carboxylates to the calcium ions of the surface, thereby directly affecting dissolution and growth. On the other hand, molecules that can form complexes in calcium ions in solution effectively alter the calcium activity and, thus, influence dissolution and growth in an indirect manner. Both effects can also be active at the same time, significantly complicating an in-depth understanding of the mode of action of these soluble additives.

Here we study the impact of the water-soluble organic molecule Congo Red (CR) on the surface morphology of calcite (10.4). CR was chosen as it has been shown to influence the crystallization of calcite.¹⁴ In the absence of CR in the solution, calcite (10.4) exhibits characteristic rhombic etch pits, which are confined by the energetically most favorable (10.4) planes and charge-neutral step edges that are oriented in the [4–4–1] and [48–1] crystallographic directions. This surface structure is drastically changed in the presence of CR. When CR is present, step edges running along the [010] direction are observed on the surface. These step edges are polar and, therefore, usually not present on the surface, because they are thermodynamically unfavored. In a time-dependent experiment, we directly follow the restructuring of an initially etch pit-covered surface into a surface that exclusively exhibits polar step edges along the [010] direction, which are decorated by CR

Received: March 20, 2015

Revised: June 5, 2015

Published: June 8, 2015

islands. Our results, thus, clearly indicate the stabilization of the otherwise thermodynamically unfavorable polar step edges by the presence of the additive.

MATERIALS AND METHODS

Congo Red (CR) was purchased from Sigma-Aldrich and used without further purification. Standard solutions of NaOH (0.1 N) and HCl (1 N) were purchased from Carl Roth. The used water was deionized using a purification setup from Millipore.

For the presented frequency modulation atomic force microscopy (FM-AFM) measurements, a modified atomic force microscope was used. The instrument has been optimized for frequency modulation imaging at the solid–liquid interface.¹⁵ All images shown here were taken in aqueous solution with a closed liquid cell (Bruker Nano Surface Division) at a constant temperature of 28 °C. The used cantilevers were gold coated and p-doped silicon (PPP-NCHAuD, Nanosensors) with an eigenfrequency of ~ 160 kHz in liquid and a spring constant of 42 N/m. The amplitude of the cantilever oscillation was kept constant at values between 0.75 and 1.75 nm. All AM-AFM images were taken with the same instrument and same cantilever types.

For each experiment, a freshly cleaved calcite crystal (Korth Kristalle GmbH) was used. After the cleavage, the crystal was cleaned by a nitrogen flow. We use a home-built sample holder that allows for clamping the calcite sample,¹⁶ thus omitting the use of adhesive tape, which might otherwise constitute a source of contaminants with unknown effect on dissolution and growth. The aqueous solutions with and without dissolved CR molecules (0.29 mM) were injected into the closed liquid cell using a syringe. Beforehand, the pH value of the solution was adjusted using NaOH (0.1 N) or HCl (1 N) to reach initial pH values of 4, 6, 9 and 11. The pH was measured with a Schott pH meter (CG 842) equipped with a BlueLine electrode from Schott. For each pH value, two samples were measured at one to three positions. Before injection, the temperature of the solution was stabilized at 30 °C. Dissolution of calcite is known to increase the pH of the solution. To estimate the change in pH, we have measured the pH change of a 10 mL solution (without CR) after immersion of a calcite crystal (58.3 mg). With a starting pH of 4.6, the pH changes to 5.2 after 1 h. After the crystal had been immersed for 21 h, the pH was 7.6. All measurements shown here were started directly (i.e., approximately 15 min) after injection of the solution. Therefore, we expect a minor increase in the pH in our measurements. However, as the results were independent of pH, this does not affect the conclusions drawn in the work.

The raw data were analyzed by using the program Gwyddion. For displaying topography images, the three-point leveling tool or the plane level tool was used. If other tools were applied such as drift correction,¹⁷ the procedure is indicated in the figure caption.

RESULTS AND DISCUSSION

Molecular Island Structure. To study the influence of the presence of CR on the calcite (10.4) surface, FM-AFM images were taken under liquid conditions at various pH values (initial pH value adjusted to 4, 6, 9, and 11). In a manner independent of the initial pH value, CR is observed to assemble at step edges, resulting in stripelike molecular islands as shown in Figure 1a. Interestingly, the observed step edges are oriented along the crystallographic [010] direction. The molecular

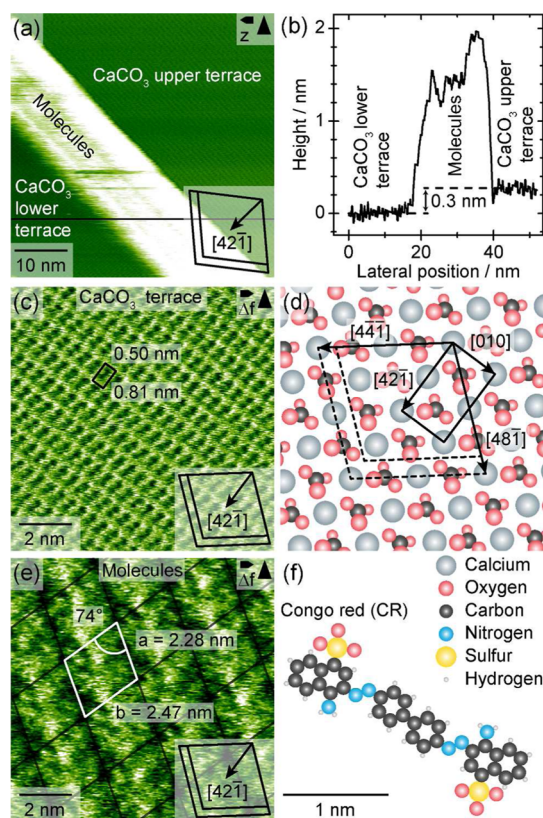


Figure 1. (a) CR forming a molecular island at a step edge running along the [010] direction, measured with FM-AFM in aqueous solution at an initial pH of 9.9. The black horizontal line indicates the position of the height profile shown in panel b. Image taken at a scan rate of 2 Hz and an amplitude of 0.85 nm. (b) Height profile showing that CR adsorbs directly at the step edge. The calcite step height of 0.3 nm is indicated. (c) High-resolution image of calcite (initial pH of 9.2), corrected for linear thermal drift and calibrated to fit the calcite surface unit cell (black rectangle). Image taken at a scan rate of 7 Hz and an amplitude of 0.85 nm. (d) Model of the calcite (10.4) surface. The calcite unit cell is indicated by a black rectangle. The typical etch pit shape (dashed parallelogram) is drawn, and the most stable step edges are marked. (e) High-resolution image obtained on a molecular island (initial pH of 9.2), corrected for linear thermal drift and calibrated with the same factors that were used for panel c. Image taken at a scan rate of 10 Hz and an amplitude of 0.85 nm. Images c and e are measured on the same sample at different positions, while image a is from a different sample with the same preparation. The white parallelogram shows the molecule unit cell. (f) Model of a CR molecule to scale with the calcite model in panel d.

islands exhibit a width in the range of 10–30 nm. Narrower islands are found at single-layer steps, while the broader islands are situated at multilayer steps. The apparent height of the islands varies between 1 and 2 nm as can be seen from a representative height profile displayed in Figure 1b. From the AFM images, the question of whether the molecules adsorb on the upper or lower side of the step edge cannot be answered.

To elucidate molecular-scale details, we acquire high-resolution FM-AFM images of the clean calcite surface and of the molecular islands on the same sample. Figure 1c shows a high-resolution image of the calcite (10.4) surface, corresponding to earlier observations in the liquid environment.¹⁸ A model of the surface is given in Figure 1d. The surface unit cell and the most stable step edges are marked in this model. In Figure 1e, the surface structure of a CR island is shown. This high-

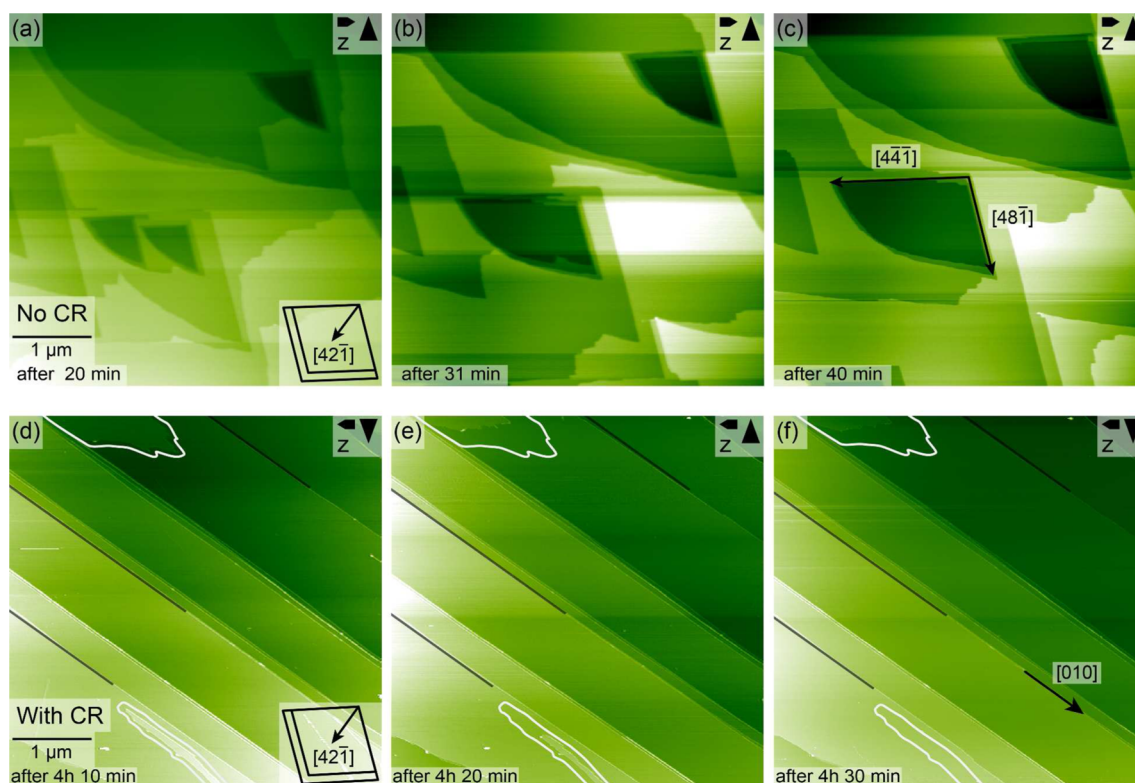


Figure 2. Image series of the calcite (10.4) surface structure in the absence (a–c) and presence (d–f) of CR at an initial pH of 4.0. (a–c) AM-AFM images taken in the absence of CR, showing that etch pits form and grow over time. During growth, they start to merge (polynomial background and line-by-line subtraction applied; scan rate of 1.5 Hz). (d–f) FM-AFM images taken in the presence of CR, where mostly step edges along the [010] direction are found (few indicated by black lines). Those steps are found to be decorated with molecular islands. Calcite terraces with irregular step edges disappear (perimeters of two shrinking islands are marked by white lines). The formation of etch pits is suppressed in the presence of CR (line-by-line subtraction applied; all images taken at a scan rate of 0.8 Hz and an amplitude of 1.68 nm).

resolution image discloses a periodic structure with a rhombic unit cell. The unit cell dimensions are as follows: $a = 2.28 \pm 0.04$ nm, and $b = 2.47 \pm 0.04$ nm. The angle between a and b is $74 \pm 1^\circ$. Interestingly, this molecular structure is not commensurate with the underlying substrate. The latter finding indicates a weak interaction of CR with the calcite terrace and might explain why CR islands do not cover the entire surface but form rather narrow molecular islands directly at steps. Moreover, this result suggests that the interaction of the molecules with the substrate is governed by, or even limited to, the interaction of the molecules with the polar step edges; i.e., the interaction is likely to be of electrostatic origin. CR (a model is shown in Figure 1f) contains two sulfonate and two amino groups, all of which can be deprotonated. Depending on the pK_a values of these functional groups, a species distribution can be calculated as a function of the actual pH, as given in the Supporting Information. At this point, we would like to address the question of a possible microscopic binding model. As shown in the Supporting Information, CR is present in five different protonation/deprotonation states. Although the composition depends on the pH, the respective minority species is present in great excess as compared to the small number of possible surface binding sites (i.e., step edge sites). Thus, given the many possibilities of the molecular species and the various possible adsorption geometries, providing a microscopic picture of CR binding would be highly speculative. Therefore, we refrain from drawing a model based solely on the AFM images.

Calcite Surface Structure in the Absence and Presence of CR.

To investigate the effect of CR on the calcite surface structure, we compare image series taken in the absence and presence of CR in the solution. These experiments were conducted at various pH values (initial values of 4, 6, 9, and 11). The obtained results are, again, independent of the actual pH value. Therefore, the image series with and without the CR additive taken at an initial pH value of 4 are shown as representative examples (Figure 2). For a better comparison, the time difference between the images was chosen such that it is nearly the same.

In the absence of CR in the solution, characteristic etch pits are known to form on calcite (10.4) with the etch pits' long diagonal oriented along the [010] direction. These etch pits are terminated by the thermodynamically most stable step edges, which are oriented along the $[48\bar{1}]$ and $[4\bar{4}\bar{1}]$ directions.^{19,20} These steps are characterized by a charge-neutral, alternating arrangement of Ca^{2+} and CO_3^{2-} ions. Consequently, there is no resulting dipole moment perpendicular to this kind of step edge.

The etch pits are observed to grow in time as is evident from a retreat of the confining step edges (Figure 2a–c). The overall shape of the pits remains, however, unchanged. Some etch pits merge into one pit.

The step edge faces span either an acute (78°) or an obtuse (102°) angle with the (10.4) plane. The steps with an obtuse angle are indicated by double lines in the pictogram in the bottom right corner of our AFM images. The dissolution velocity at steps with an acute angle is lower than the velocity at

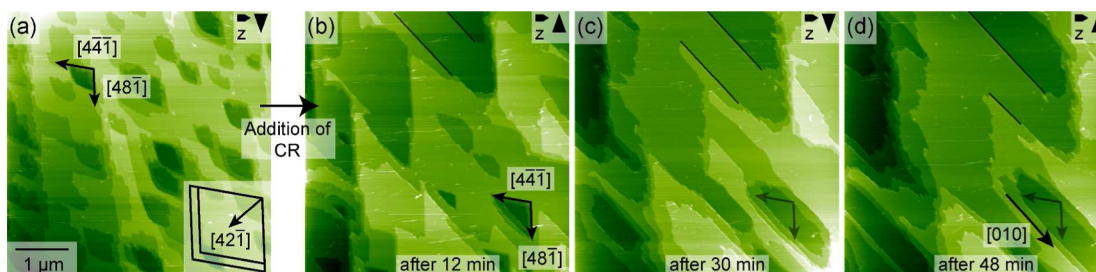


Figure 3. Time-resolved formation of step edges along the $[010]$ direction. (a) Etch pits on the calcite (10.4) surface in the absence of CR. (b) After CR had been added to the solution, etch pits change their appearance to a triangular shape. (c and d) Over time, the triangular etch pits disappear and exclusively step edges along the $[010]$ direction (some indicated by black lines) prevail. All images taken at a scan rate of 1 Hz and an amplitude of 0.90 nm.

steps with an obtuse angle.¹⁹ Thus, the dissolution is known to be anisotropic and caused by different dissolution velocities for acute and obtuse steps. This asymmetry has been discussed as the origin of the fact that the etch pits are not symmetrically shaped but exhibit a rounded corner.²⁰ Liang and Baer suggest that etch pit nucleation is initiated by thermal events or single-point defects on the surface.¹⁹ Therefore, the density and position of the etch pits appear to be somewhat random in the AFM images.

In the presence of CR, the surface structure is drastically different. No characteristic etch pits are present on the surface. After some time, the step edges are no longer oriented along the $[48\bar{1}]$ and $[4\bar{4}\bar{1}]$ directions, but exclusively along the $[010]$ direction. If step edges are considered with unequal ion composition, the step edges exhibit a resulting dipole moment; i.e., they are polar and, thus, less stable than nonpolar steps.²¹ Such polar step edges can, e.g., be found along the $[010]$ and $[42\bar{1}]$ directions. Along these directions, the edges are composed of one type of ion solely, i.e., either Ca^{2+} or CO_3^{2-} ions. Because of their high dipole moment, these steps do not exist in the absence of additive molecules. These polar step edges are all observed to be decorated by CR islands. Interestingly, the CR-decorated step edges do not change over time (Figure 2d–f). This is in sharp contrast to step edges that are oriented in other directions (white lines). The latter edges exhibit no CR decoration, and we observe the retreat of these edges, resulting in a surface that exclusively exhibits step edges along the $[010]$ direction.

Change in Calcite Surface Structure upon Addition of CR. The different surface structures obtained in the absence and presence of CR can be controlled by thermodynamics or kinetics. In other words, the absence of the otherwise stable step edges oriented along the $[48\bar{1}]$ and $[4\bar{4}\bar{1}]$ directions and the presence of the polar step edges could indicate that the polar step edges become thermodynamically favored. An alternative explanation would, however, be that the step edges oriented along the $[48\bar{1}]$ and $[4\bar{4}\bar{1}]$ directions remain thermodynamically favorable, but their formation is kinetically hindered when CR is present, decorating the $[010]$ steps.

To clarify the effect of CR on the thermodynamics of the calcite surface, we start with a calcite (10.4) sample that is initially covered by etch pits and follow the changes that are induced by the addition of CR during the FM-AFM measurement (Figure 3). The experiment is started without a CR additive at an initial pH value of 4 (Figure 3a). As expected, the etch pits show a rhombic shape, where one corner formed by the acute steps is rounded. We then exchanged the CR-free

solution with a solution containing dissolved CR molecules at a pH value of 4. This solution exchange was done without stopping the measurement. The series of images shown in Figure 3b–d starts 12 min after the solution has been exchanged. As is evident from these FM-AFM images, the etch pits start to change their geometry upon addition of CR. The pits no longer appear with rhombic geometry but rather exhibit a triangular shape with step edges along the $[010]$, $[48\bar{1}]$, and $[4\bar{4}\bar{1}]$ directions. After 30 min, most steps along the $[48\bar{1}]$ and $[4\bar{4}\bar{1}]$ directions have disappeared. Instead, the surface now predominantly exhibits step edges along the $[010]$ direction. Continuing this experiment results in a surface that exclusively exhibits step edges along the $[010]$ direction as shown in Figure 2f. This result clearly demonstrates that the polar step edges along the $[010]$ direction become thermodynamically favored as compared to the usually most stable steps along the $[48\bar{1}]$ and $[4\bar{4}\bar{1}]$ directions. This might originate from a competitive binding of CR to the five different step edges discussed here. We can speculate that the CR binding to the polar step edges is stronger, thus eventually favoring these edges. In an additional experiment (not shown), we exchanged the CR solution in the liquid cell several times with Milli-Q water, but we were not able to remove the CR molecule adsorbed on the surface. Thus, we can conclude that the binding of the molecules to the polar $[010]$ step edges is, indeed, rather firm.

CONCLUSION

The effect of CR on the surface structure of the most stable cleavage plane of calcite, calcite (10.4), is studied using high-resolution FM-AFM in liquids. In the absence of CR, characteristic etch pits exist on the surface, which are terminated by the thermodynamically most stable, charge-neutral step edges along the $[48\bar{1}]$ and $[4\bar{4}\bar{1}]$ surface directions. In contrast, in the presence of CR, no etch pits exist on the surface, but we observe the existence of polar $[010]$ step edges that are stable over time. These step edges are decorated by molecular islands, indicating that the adsorption of the molecules at the step edges stabilizes the polar step edge. Interestingly, no other step edges remain on the surface. This finding is independent of the pH value in the pH range studied here. As CR contains polar and ionic functional groups, namely, two amino groups and two sulfonate groups, we can envision that the stabilization mechanism is based on electrostatic interaction. The details of the interaction mechanism, e.g., whether calcium-terminated step edges are stabilized by the adsorption of the sulfonate group or carbonate-terminated step edges by the adsorption of the amino groups, or both, cannot

be finalized on the basis of the FM-AFM experiments presented here.

The fact that a drastic surface morphology change can be observed after addition of a CR solution illustrates that the CR-decorated polar step edges along the [010] direction become thermodynamically favored over the otherwise most stable edges found along the [48-1] and [4-4-1] directions.

As exclusively polar step edges along the [010] direction remain on the surface, this study might pave the way for a rational design of molecules for additive-controlled crystallization.

■ ASSOCIATED CONTENT

Supporting Information

CR species distribution as a function of pH. The Supporting Information is available free of charge on the ACS Publications website at DOI: 10.1021/acs.langmuir.5b01043.

■ AUTHOR INFORMATION

Corresponding Author

*E-mail: kuehnle@uni-mainz.de.

Notes

The authors declare no competing financial interest.

■ ACKNOWLEDGMENTS

Stimulating discussions with Martin Schreiber are gratefully acknowledged. We thank Stefanie Klassen for assistance during the data acquisition.

■ ABBREVIATIONS

AFM, atomic force microscopy; FM, frequency modulation; CR, Congo Red

■ REFERENCES

- (1) Song, R.-Q.; Cölfen, H. Additive controlled crystallization. *CrystEngComm* **2011**, *13* (5), 1249–1276.
- (2) Sangwal, K. *Additives and Crystallization Processes: From Fundamentals to Applications*; Wiley VCH: Berlin, 2007.
- (3) Deer, W. A.; Howie, R. A.; Zussman, J. *An introduction to the rock-forming minerals*; Longman Scientific & Technical: Harlow, U.K., 1992.
- (4) Meldrum, F. C. Calcium carbonate in biomineralisation and biomimetic chemistry. *Int. Mater. Rev.* **2003**, *48* (3), 187–224.
- (5) Nudelman, F.; Sommerdijk, N. A. J. M. Biomineralization as an Inspiration for Materials Chemistry. *Angew. Chem., Int. Ed.* **2012**, *51* (27), 6582–6596.
- (6) Orme, C. A.; Noy, A.; Wierzbicki, A.; McBride, M. T.; Grantham, M.; Teng, H. H.; Dove, P. M.; DeYoreo, J. J. Formation of chiral morphologies through selective binding of amino acids to calcite surface steps. *Nature* **2001**, *411*, 775–779.
- (7) Nelea, V.; Chien, Y.-C.; Paquette, J.; McKee, M. D. Effects of Full-Length Phosphorylated Osteopontin and Constituent Acidic Peptides and Amino Acids on Calcite Dissolution. *Cryst. Growth Des.* **2014**, *14* (3), 979–987.
- (8) Kim, I. W.; Giocondi, J. L.; Orme, C.; Collino, S.; Evans, J. S. Morphological and kinetic transformation of calcite crystal growth by prismatic-associated asprich sequences. *Cryst. Growth Des.* **2008**, *8* (4), 1154–1160.
- (9) Sand, K. K.; Pedersen, C. S.; Sjoberg, S.; Nielsen, J. W.; Makovicky, E.; Stipp, S. L. S. Biomineralization: Long-Term Effectiveness of Polysaccharides on the Growth and Dissolution of Calcite. *Cryst. Growth Des.* **2014**, *14* (11), 5486–5494.
- (10) Fukuma, T.; Kobayashi, K.; Matsushige, K.; Yamada, H. True atomic resolution in liquid by frequency-modulation atomic force microscopy. *Appl. Phys. Lett.* **2005**, *87* (3), 034101.

(11) Higgins, M. J.; Riener, C. K.; Uchihashi, T.; Sader, J. E.; McKendry, R.; Jarvis, S. P. Frequency modulation atomic force microscopy: A dynamic measurement technique for biological systems. *Nanotechnology* **2005**, *16* (3), S85–S89.

(12) Meyer, E.; Jarvis, S. P.; Spencer, N. D. Scanning probe microscopy in materials science. *MRS Bull.* **2004**, *29* (7), 443–448.

(13) Fukuma, T.; Onishi, K.; Kobayashi, N.; Matsuki, A.; Asakawa, H. Atomic-resolution imaging in liquid by frequency modulation atomic force microscopy using small cantilevers with megahertz-order resonance frequencies. *Nanotechnology* **2012**, *23* (13), 12.

(14) Kohlschütter, V.; Egg, C. Über Wirkungen von Farbstoffzusätzen auf die Krystallisation des Calciumcarbonats. *Helv. Chim. Acta* **1925**, *8*, 697–703.

(15) Rode, S.; Stark, R.; Lübke, J.; Tröger, L.; Schütte, J.; Umeda, K.; Kobayashi, K.; Yamada, H.; Kühnle, A. Modification of a commercial atomic force microscopy for low-noise, high-resolution frequency-modulation imaging in liquid environment. *Rev. Sci. Instrum.* **2011**, *82* (7), 073703.

(16) Tröger, L.; Schütte, J.; Ostendorf, F.; Kühnle, A.; Reichling, M. Concept for support and cleavage of brittle crystals. *Rev. Sci. Instrum.* **2009**, *80* (6), 063703.

(17) Rahe, P.; Bechstein, R.; Kühnle, A. Vertical and lateral drift corrections of scanning probe microscopy images. *J. Vac. Sci. Technol., B: Nanotechnol. Microelectron.: Mater., Process., Meas., Phenom.* **2010**, *28* (3), C4E31–C4E38.

(18) Rode, S.; Oyabu, N.; Kobayashi, K.; Yamada, H.; Kühnle, A. True Atomic-Resolution Imaging of (10–14) Calcite in Aqueous Solution by Frequency Modulation Atomic Force Microscopy. *Langmuir* **2009**, *25* (5), 2850–2853.

(19) Liang, Y.; Baer, D. R. Anisotropic dissolution at the CaCO₃(1014)-water interface. *Surf. Sci.* **1997**, *373* (2–3), 275–287.

(20) Britt, D. W.; Hlady, V. In-situ atomic force microscope imaging of calcite etch pit morphology changes in undersaturated and 1-hydroxyethylidene-1,1-diphosphonic acid poisoned solutions. *Langmuir* **1997**, *13* (7), 1873–1876.

(21) Ruiz-Agudo, E.; Kowacz, M.; Putnis, C. V.; Putnis, A. The role of background electrolytes on the kinetics and mechanism of calcite dissolution. *Geochim. Cosmochim. Acta* **2010**, *74* (4), 1256–1267.